2012;69:765-8.

[16] Alsalem A, Shaheen R, Alkuraya FS. Vanishing white matter disease caused by EIF2B2 mutation with the presentation of an adrenoleukodystrophy phenotype. Gene 2012;496:141-3.

[17] van der Knaap MS, Kamphorst W, Barth PG, Kraaijeveld CL, Gut E, Valk J. Phenotypic variation in leukoencephalopathy with vanishing white matter. Neurology 1998;51:540-7.

[18] Yamamoto T, Nanba E, Ninomiya H, Higaki K, Taniguchi M, Zhang H, et al. NPC1 gene mutations in Japanese patients with Niemann-Pick disease type C. Hum Genet 1999;105:10-6.

[19] Shimojima K, Komoike Y, Tohyama J, Takahashi S, Paez MT, Nakagawa E, et al. TULIP1 (RALGAPA1) haploinsufficiency with brain development delay. Genomics 2009;94:414-22.

[20] Kumar P, Henikoff S, Ng PC. Predicting the effects of coding non-synonymous variants on protein function using the SIFT algorithm. Nat Protoc 2009;4:1073-81.

[21] Adzhubei IA, Schmidt S, Peshkin L, Ramensky VE, Gerasimova A, Bork P, et al. A method and server for predicting damaging missense mutations. Nat Methods 2010;7:248-9.

[22] Kircher M, Witten DM, Jain P, O'Roak BJ, Cooper GM, Shendure J. A general framework for estimating the relative pathogenicity of human genetic variants. Nat Genet 2014;46:310-5.

[23] Shimojima K, Narita A, Maegaki Y, Saito A, Furukawa T, Yamamoto T. Whole-exome sequencing identifies a de novo TUBA1A mutation in a patient with sporadic malformations of cortical development: a case report. BMC Res Notes

2014;7:465.

[24] Fogli A, Schiffmann R, Bertini E, Ughetto S, Combes P, Eymard-Pierre E, et al. The effect of genotype on the natural history of eIF2B-related leukodystrophies. Neurology 2004;62:1509-17.

[25] Matsukawa T, Wang X, Liu R, Wortham NC, Onuki Y, Kubota A, et al. Adult-onset leukoencephalopathies with vanishing white matter with novel missense mutations in EIF2B2, EIF2B3, and EIF2B5. Neurogenetics 2011;12:259-61.

[26] Shimada S, Miya K, Oda N, Watanabe Y, Kumada T, Sugawara M, et al. An unmasked mutation of EIF2B2 due to submicroscopic deletion of 14q24.3 in a patient with vanishing white matter disease. Am J Med Genet A 2012;158A:1771-7.

[27] van der Lei HD, Steenweg ME, Barkhof F, de Grauw T, d'Hooghe M, Morton R, et al. Characteristics of early MRI in children and adolescents with vanishing white matter. Neuropediatrics 2012;43:22-6.

[28] Scheper GC, van der Knaap MS, Proud CG. Translation matters: protein synthesis defects in inherited disease. Nat Rev Genet 2007;8:711-23.

[29] Pavitt GD. eIF2B, a mediator of general and gene-specific translational control. Biochem Soc Trans 2005;33:1487-92.

[30] Liu R, van der Lei HD, Wang X, Wortham NC, Tang H, van Berkel CG, et al. Severity of vanishing white matter disease does not correlate with deficits in eIF2B activity or the integrity of eIF2B complexes. Hum Mutat 2011;32:1036-45.

[31] van der Voorn JP, van Kollenburg B, Bertrand G, Van Haren K, Scheper GC, Powers JM, et al. The unfolded protein response in vanishing white matter disease. J Neuropathol Exp Neurol 2005;64:770-5.

[32] Bugiani M, Boor I, Powers JM, Scheper GC, van der Knaap MS.

Leukoencephalopathy with vanishing white matter: a review. J Neuropathol Exp Neurol 2010;69:987-96.

[33] Kantor L, Pinchasi D, Mintz M, Hathout Y, Vanderver A, Elroy-Stein O. A point mutation in translation initiation factor 2B leads to a continuous hyper stress state in oligodendroglial-derived cells. PLoS One 2008;3:e3783.

Figure legend

Figure 1. Brain MRI findings of the patients examined. Axial images show various degrees of abnormal white matter. A and B; Patient 1 examined at 60 years of age. C and D; Patient 2 examined at 3 years of age. E and F; Patient 3 examined at 8 months of age. G and H; Patient 4 examined at 13 years of age. I and J; patient 5 examined at 16 years of age. K and L; patient 6 examined at 13 months of age. T1-weighted axial images (A, E, G, and I) and T2-weigthed axial images (B-D, F, H, and J-L). Periventricular zones of patient 1 are not distinguished (A and B). T2-high intensity is only shown in deep white matter, indicating early disease stage in patient 4 and 5 (H and J, respectively).

Figure 2. Schematic representation of the distribution of EIF2B gene mutations. The novel mutations identified in this study are depicted on the primary structures of EIF2B genes in red characters, while known mutations are shown in black.

Supplemental Figure 1. Electropherograms. Electropherograms of the mutations identified in this study are presented.

Supplemental Figure 2. Conservation among species. The positions of the identified nucleotide mutations (red arrows) and the three neighboring amino-acids sequences are shown in the UCSC Genome Browser. All altered amino-acids are conserved among mammalians.

Figure 1
Click here to download high resolution image

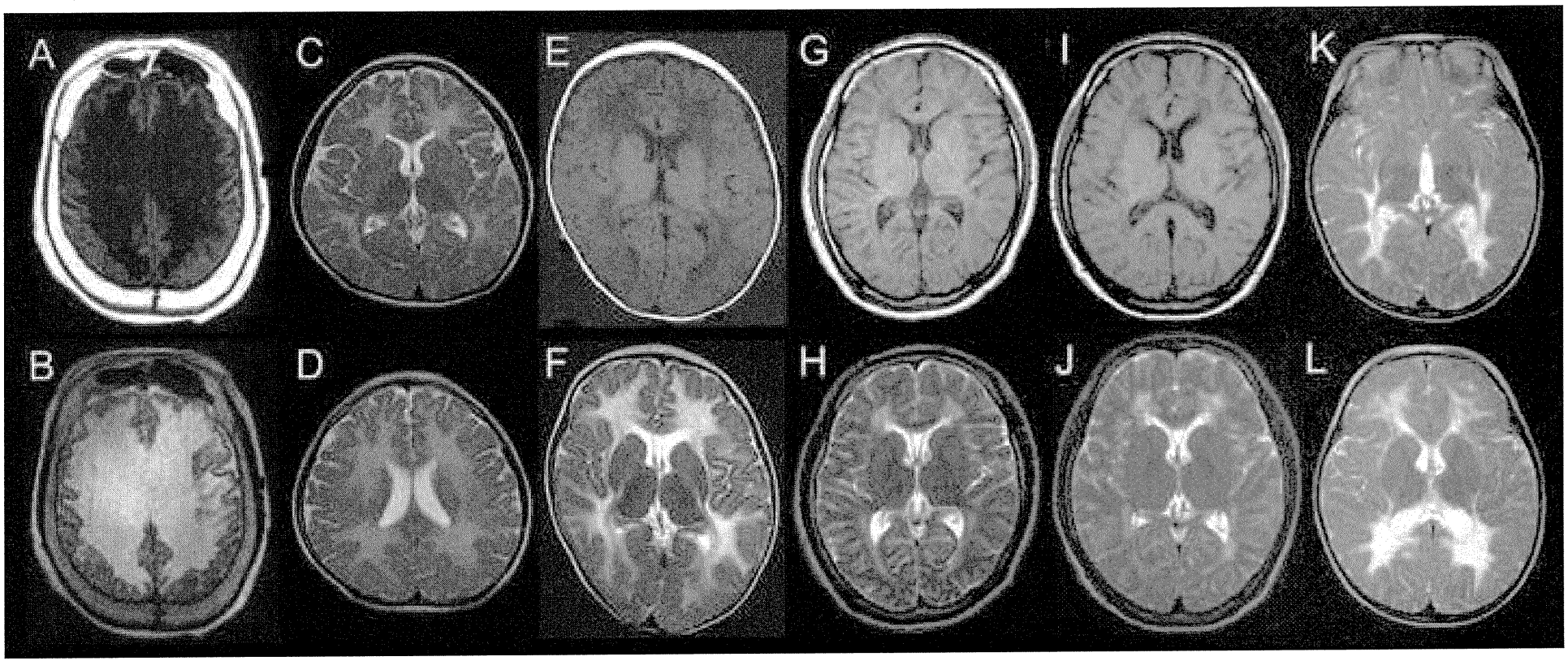

Table 1

Table 1. Summaries of the clinical information of the patients and the results of mutation analyses

Patients	Patient 1	Patient 2	Patient 3		Patient 4		Patient 5		Patient 6	
Clinical information										
Gender	F	F	M		M		M		M	
Present age (y/m)	61y	8y	8m		22y		19y		5y5m	
Onset age (y/m)	29y	3y	8m		13y		13y		13m	
Provoking event	-	Infection	Infection (fever)		Lack of sleep		Head trauma		Infection (fever)	
Seizure	+	+	+		+		-		+	
Disturbed consciousness	+	+	+		-		+		+	
Other neurological findings	Bedridden	Bulbar paralysis	Spasticity, developmental delay		Mild ataxia		Muscular weakness		Gait disturbance	
Consanguinity	+	-	-		-		-		-	
Family history	-	-	-		The elder brother of Pt.5		The younger brother of Pt.4		-	
Identified mutations										
Genes	*EIF2B1*	*EIF2B2*	*EIF2B2*		*EIF2B4*		*EIF2B4*		*EIF2B5*	
Chromosomal location	12q24.31	14q24.3	14q24.3		2p23.3		2p23.3		3q27.1	
Inheritance	Homozygous	Homozygous	Compound heterozygous		Compound heterozygous		Compound heterozygous		Compound heterozygous	
Exon	exon 8	exon 2	exon 2	exon 5	exon 6	exon 11	exon 6	exon 11	exon 7	exon 7
Nucleotide alteration	c.715T>G	c.254T>A	c.254T>A	c.682A>G	c.556T>A	c.1070G>A	c.556T>A	c.1070G>A	c.915G>A	c.1154T>C
Amino-acid change	p.F239V	p.V85E	p.V85E	p.R228G	p.Y186N	p.R357Q	p.Y186N	p.R357Q	p.M305I	p.I385T
Novel/recurrent	Novel	Recurrent	Recurrent	Novel	Novel	Recurrent	Novel	Recurrent	Novel	Novel
Origin	Not confirmed	Both parents	Paternal	Maternal	Maternal	Paternal	Maternal	Paternal	de novo	Maternal
dbSNP build 138	-	-	-	-	-	rs113994033	-	rs113994033	-	-
Damaging prediction										
SIFT score	0.12	0.00	0.00	0.00	0.25	0.15	0.25	0.15	0.13	0.00
SIFT prediction	T	D	D	D	T	T	T	T	T	D
Polyphen2 HVAR score	0.715	0.995	0.995	0.999	0.979	0.637	0.979	0.637	0.196	0.95
Polyphen2 HVAR prediction	P	D	D	D	D	P	D	P	B	D
CADD score (raw)	5.436	5.264	5.264	3.760	4.290	5.227	4.290	5.227	3.735	4.732
CADD score (PHRED-like)	35.0	33.0	33.0	19.1	22.4	33.0	22.4	33.0	19.0	26.4

F, female; M, male; y, years; m, months; Pt., Patient; HVAR, HumVar-trained model autosomal recessive pattern; T, tolerate; D, damaging; B, benign

Figure 2
Click here to download high resolution image